Epigenetic ALYREF/UHRF1/RHOB Axis in Corneal Wound Healing and Implications for Epithelial Tumorigenesis

Hua Zhang,[1] Shuning Lan,[1] Disuo Ren,[2] Xiaoyan Chen,[1] Yong Lin,[1] Qiongjie Cao,[1] Weiwei Xu,[1] Jiao Wang,[1] Peter Sol Reinach,[1] Dongsheng Yan,[1] and Guangying Luo[1]

[1]State Key Laboratory of Eye Health, Eye Hospital, Wenzhou Medical University, Wenzhou, China
[2]The First Affiliated Hospital of Wenzhou Medical University, Wenzhou, China

Correspondence: Guangying Luo, School of Ophthalmology and Optometry, Eye Hospital, Wenzhou Medical University, No. 270, Xueyuan West Rd., Wenzhou, Zhejiang Province 325027, China; lgyszr@126.com or luoguangying@wmu.edu.cn. Dongsheng Yan, School of Ophthalmology and Optometry, Eye Hospital, Wenzhou Medical University, No. 270, Xueyuan West Rd., Wenzhou, Zhejiang Province 325027, China; dnaprotein@hotmail.com or yandsh@eye.ac.cn.

Received: December 2, 2024
Accepted: March 3, 2025
Published: March 25, 2025

Citation: Zhang H, Lan S, Ren D, et al. Epigenetic ALYREF/UHRF1/RHOB axis in corneal wound healing and implications for epithelial tumorigenesis. *Invest Ophthalmol Vis Sci.* 2025;66(3):54. https://doi.org/10.1167/iovs.66.3.54

Purpose. Corneal epithelial wound healing (CEWH) is a complex process influenced by epigenetic regulation. Ubiquitin-like with plant homeodomain (PHD) and ring finger domains 1 (UHRF1), it plays a key role in integrating epigenetic signals. However, its precise function in modulating CEWH remains poorly understood. We describe here the functional mechanisms of UHRF1 in modulating CEWH.

Methods. Quantitative Reverse Transcription PCR (RT-qPCR), immunofluorescence, and gene manipulation were used to investigate UHRF1 expression patterns and functions during CEWH. Integrated multi-omics and targeted bisulfite sequencing (TBS) were performed to reveal the downstream target of UHRF1. Mutation assay was used to examine whether Aly/REF export factor (ALYREF) can recognize and bind RNA m^{5}C-*UHRF1*. Gene expression profiling interactive analysis (GEPIA) was utilized to validate the correlation of UHRF1 with its upstream and downstream targets.

Results. In this study, we demonstrate that UHRF1 enhances CEWH and sustains DNA methylation during CEWH, which is essential for this effect. A multi-omics analysis identified Ras homolog family member B (RHOB) as a downstream target of UHRF1. Our findings further revealed that UHRF1 epigenetically downregulates RHOB, thereby facilitating CEWH. Moreover, we showed that ALYREF binds to m^{5}C sites on UHRF1 mRNA and enhances its translation. Finally, our analysis of molecular alterations and the clinical significance of ALYREF, UHRF1, and RHOB expression suggests that this epigenetic axis is also relevant in epithelial-derived tumors, which represent approximately 90% of all tumors.

Conclusions. Our study identifies a novel epigenetic ALYREF/UHRF1/RHOB axis that enhances CEWH. Importantly, this axis appears to be conserved across various epithelial-derived tumors, suggesting its broader biological significance.

Keywords: ALYREF, corneal epithelial wound healing (CEWH), epithelial tumors, RHOB, UHRF1

The renewal of the corneal epithelial layer is critical for maintaining its integrity and transparency, both of which are essential for preserving normal vision.[1] A key function of this process is the preservation of the tight junctional barrier, which prevents pathogenic infiltration into the tissue.[2] Various environmental challenges, such as physical trauma or pathogen invasion, can trigger the corneal epithelial renewal process.[3] This injury-induced response, known as corneal epithelial wound healing (CEWH), involves the activation and migration of limbal stem cells to repair the damaged epithelial layer.[4] CEWH is a vital adaptive response, reducing the time needed to mitigate the effects of epithelial damage in ocular surface diseases.[5,6] In recent years, epigenetics-linking environmental stimuli to physiological outcomes has gained growing attention for its role in regulating CEWH.[7]

Recent studies have shown that CEWH is governed by an orchestrated epigenetic regulatory process involving an orchestrated program of cell differentiation, proliferation, migration, and tissue remodeling.[8] The key mechanisms include DNA methylation, histone modification, and non-coding RNA regulation, all of which modulate the CEWH process.[9–11] In particular, RNA m^{5}C modification has emerged as a crucial regulator of the CEWH response following injury.[12] The RNA methylase NOP2/Sun domain family member 2 (NSUN2) mediates m^{5}C modification of the ubiquitin-like containing plant homeodomain (PHD) and really interesting new gene (RING) finger domains 1 (UHRF1) mRNA, regulating its expression to promote corneal epithelial cell proliferation and migration.[12] UHRF1, a well-known epigenetic integrator, plays a critical role

in coordinating DNA methylation and histone modification during this process.[13,14]

UHRF1 was initially identified as a novel nuclear protein highly expressed in proliferating cells.[15] Functional assays revealed that UHRF1 promotes malignant phenotype and tissue regeneration.[16–18] Numerous studies have established UHRF1 as an oncogene in various cancers.[19] Structurally, UHRF1 comprises five domains—ubiquitin-like domain (UBL), tandem Tudor domain (TTD), PHD, RING domain, and SET and RING-associated domain (SRA)—each of which contributes to its function in DNA methylation and histone modification.[2] In mice, the DNA methylation and histone modification are dynamic changes that are involved in CEWH.[9,10] In mouse models, UHRF1 expression is significantly upregulated in the injured corneal epithelium within 48 hours,[12] reinforcing its role as an epigenetic integrator during CEWH. Despite previous findings that UHRF1 is regulated by RNA m^5C modification via NSUN2,[12] the precise mechanisms by which UHRF1 modulates CEWH remain unclear.

This study aims to elucidate these mechanisms by demonstrating that UHRF1 maintains DNA methylation during CEWH. Multi-omics analysis identifies the small GTP-binding protein Ras homolog family member B (RHOB) as a downstream target of UHRF1. The UHRF1 epigenetically downregulates RHOB to promote CEWH. In addition, UHRF1 is recognized and regulated by the RNA m^5C reader, Aly/REF export factor (ALYREF). Our results present a novel epigenetic ALYREF/UHRF1/RHOB axis during CEWH, which may have broader implications for epithelial-derived tumors, as approximately 90% of human cancers originate from epithelial tissues.[20]

Materials and Methods

Mice and CEWH Model

Six-week-old C57BL/6 mice were obtained from the Beijing Vital River Co. and bred at the Wenzhou Medical University Experimental Animal Center. All animal experiments were performed in compliance with the ARVO Statement for the Use of Animals in Ophthalmic and Vision Research and approved by the Wenzhou Medical University Animal Care and Use Committee.

Mice were subjected to CEWH experiments following previously established protocols.[12] After the mice were anesthetized, a corneal rust ring remover (The Alger Company, Inc., Lago Vista, TX, USA) was used to scrape away the epithelial layer within a defined circular area on the right eye, designating this as the wound healing (WH) group, whereas the left eye remained untreated as the healthy control (CT) group. Tissue samples were collected at 24, 48, and 72 hours for molecular analyses.

Cell Culture and Gene Manipulation

Human corneal epithelial cells (HCECs) were generously provided by Araki Sasaki from the Miyata Eye Clinic in Kagoshima, Japan. The cells were cultured in DMEM/F12 medium (Invitrogen, Carlsbad, CA, USA) supplemented with 10% fetal bovine serum (FBS; Invitrogen) and maintained at 37°C in a 5% CO_2 atmosphere. For gene manipulation, HCECs were transfected with specific siRNAs to silence target genes or overexpressed using lentiviral transfection, with modified plasmids introduced into HCECs via HitransG P (Genechem Co., Ltd., Shanghai, China). These genetically modified HCECs were subsequently used for functional assays and molecular biology studies.

Western Blot

Total protein was extracted from the mouse corneal epithelium or HCECs using a RIPA lysis buffer (Beyotime, Shanghai, China). Protein concentrations were measured using a SpectraMax M5 microplate reader (Molecular Devices, San Jose, CA, USA) at 562 nm. Proteins were then separated by sodium dodecyl sulfate-polyacrylamide gel electrophoresis (SDS-PAGE) based on molecular weight. The separated proteins were transferred onto a nitrocellulose membrane and probed with primary antibodies-mouse anti-UHRF1 (1:1000; Santa Cruz), rabbit anti-RHOB (1:1000; Proteintech), rabbit anti-Aly/Ref (1:1000; Abcam), or rabbit anti-β-actin (1:1000; Abcam) overnight at 4°C. After primary antibody incubation, the membranes were treated with IRDye 800CW fluorescent secondary antibody (1:5000; LI-COR Biosciences). Target protein bands were detected with the Odyssey CLx imaging system (Gene Company Limited, USA) and quantified using ImageJ software.

Dot Blot

The total DNA of HCECs was purified using the DNeasy Blood & Tissue Kit (QIAGEN GmbH, Germany). One microgram of DNA was denatured, crosslinked to a nylon membrane using ultraviolet (UV) light, and blocked with 5% fat-free milk. We incubated the membrane overnight at 4°C with an anti-m^5C antibody (1:1000; Diagenode, Denville, NJ, USA; C15200081), then applied horseradish peroxidase-conjugated secondary antibodies (1:3000; CST, 7076) for further incubation. The m^5C content was visualized and analyzed using AlphaView FluorChemQ (ProteinSimple, Santa Clara, CA, USA).

Immunofluorescence

Frozen tissue sections were fixed, permeabilized, and blocked with 5% goat serum. The sections were then incubated overnight at 4°C with primary rabbit anti-UHRF1 antibodies (1:200; CST, D6G8E), followed by incubation with horseradish peroxidase-conjugated secondary antibodies (1:400; CST, 7076). After antibody staining, the sections were counterstained with DAPI (Beyotime; P0131) and mounted. The processed sections were visualized using a DM4B upright fluorescence microscope (Leica) and analyzed with ImageJ software.

EdU Assay

HCECs were seeded on 14 mm round cell slides and transfected with siRNA or infected with lentivirus the following day. After 48 hours, the cells were fixed, permeabilized, and blocked. The Click-iT EdU Alexa Fluor 594 Imaging Kit (Invitrogen; C10339) was used to assess the proliferative activity of the treated HCECs. The slides were then counterstained with DAPI (Beyotime; P0131) and mounted. Finally, the cell slides were visualized using a DM4B upright fluorescence microscope (Leica) and analyzed with ImageJ software.

Investigative Ophthalmology & Visual Science

Scratch Wound Assay

HCECs were seeded in 12-well plates and transfected with siRNA or infected with lentivirus on the following day, once the cell layers reached confluence. A scratch was created along the center of each well using a 100 µL pipette tip. Images were taken at 0 and 24 hours using a microscope (Zeiss) to assess wound closure. Migratory activity of the HCECs was subsequently analyzed with ImageJ software.

Quantitative Reverse Transcription PCR

Total RNA was extracted from mouse corneal epithelium or HCECs using Trizol Reagent, followed by purification through chloroform/isopropanol extraction and ethanol precipitation. RNA concentrations were assessed using a NanoDrop ND-100 (Thermo Fisher Scientific). Five hundred nanograms of RNA were reverse transcribed into cDNA, and target gene expression levels were determined using QuantStudio 5 (ABI, Singapore) and the SYBR Green method.

Plasmids

To investigate the role of RNA m^5C in UHRF1 expression, expression plasmids UHRF1 wild type (WT) and UHRF1 mutant (MUT; C147G, C969G, C970G, C1039G, C1272G, and C1456G) were constructed via cloning the UHRF1 gene into pcDNA 3.1 vector (Vector Builder, China).[12] Similarly, to examine the role of ALYREF K171 in recognizing m^5C-modified UHRF1 transcripts, expression plasmids ALYREF WT and ALYREF MUT (K171A) were cloned into pRP[Exp]-EGFP/Puro vector (Vector Builder, China).[21]

Luciferase Activity Assay

HEK293T cells were seeded in 24-well plates, and when cell confluence reached 90%, plasmids were transfected using Lipofectamine 2000. Six hours post-transfection, the medium was replaced with a fresh, serum-containing medium. After 48 hours, cells were lysed, and the supernatant was then placed in a 96-well white plate. Luciferase activity was measured at 560 nm using a microplate reader.

Reduced Representation Bisulfite Sequencing

Genomic DNA was extracted and prepared for the reduced representation bisulfite sequencing (RRBS) library construction using the Acegen Rapid RRBS Library Prep Kit (Acegen, Cat. No. AG0422) according to the manufacturer's instructions. Briefly, 100 ng of genomic DNA was digested with MspI, end-repaired, 3′-dA-tailed, and ligated to 5-methylcytosine-modified adapters. Following bisulfite treatment, the DNA was amplified via 12 cycles of PCR with Illumina 8-bp dual index primers. Size selection was conducted to isolate DNA fragments ranging from 100 to 350 bp, resulting from MspI digestion, using a dual-SPRI protocol as specified by the manufacturer. The RRBS libraries were sequenced on an Illumina platform with a 150 × 2 paired-end sequencing protocol.

We used BSMAP version 2.7.3 to align the clean reads to the reference genome, and methylation levels at individual sites were determined with the same software. Differentially methylated regions (DMRs) were identified using metilene v0.2-8, which applies a binary segmentation algorithm coupled with Mann-Whitney U (MWU) and 2D Kolmogorov-Smirnov (KS) statistical tests to detect DMRs between sample pairs or groups. Final DMRs were obtained after applying multiple testing corrections. Functional enrichment analysis of DMRs involved examining overlapping genomic regions as well as adjacent upstream and downstream areas. We used Gene Ontology (GO) analysis to determine biological processes associated with DMRs, and Kyoto Encyclopedia of Genes and Genomes (KEGG) analysis provided insights into protein interaction networks and cellular pathways.

Targeted Bisulfite Sequencing

Gene-specific DNA methylation was evaluated using next-generation sequencing-based bisulfite sequencing (BSP), following previously established protocols.[22] Targeted BSP libraries were prepared with the Acegen Targeted Methyl Panel Kit (Acegen, Cat. No. AG0508) according to the manufacturer's instructions. Briefly, BSP primers were designed using an Acegen custom script, and 500 ng of genomic DNA was converted with the ZYMO EZ DNA Methylation-Gold Kit (Zymo Research, Irvine, CA, USA). The converted DNA served as a template for PCR amplification with 10 cycles. PCR products from multiple genes for each sample were end-repaired, 3′-dA-tailed, and ligated to 5-methylcytosine-modified adapters. Libraries were sequenced on Illumina platforms with a 150 × 2 paired-end sequencing protocol.

Target sequences were mapped using BSMAP version 2.7.3, which was also used to determine methylation levels at various sites on the amplicons. Methylated cytosine sites were quantified in the CG context. To analyze intergroup differences, we performed a *t*-test to compare methylation levels across different amplicon groups.

Statistical Analysis

Each experiment was repeated at least three times. All data in this study are expressed as the mean ± SEM. Statistical differences were performed by two-tailed Student's *t*-test or 2-way ANOVA. The result significance is denoted with the indicated number of asterisks ($^*P < 0.05$, $^{**}P < 0.01$, $^{***}P < 0.001$).

Results

Temporal and Spatial Expression Patterns of UHRF1

Our previous study indicated that UHRF1 is involved in mediating CEWH,[12] but its specific function remained unclear. To address this, we assessed the temporal and spatial expression patterns of UHRF1 during CEWH. Through RT-qPCR and immunofluorescence, we tracked UHRF1 expression levels at 24, 48, and 72 hours post-wounding. UHRF1 is predominantly localized to basal corneal epithelial cells, and its expression showed a significant increase after injury, peaking at 48 hours before declining slightly at 72 hours (Figs. 1A–C, Supplementary Fig. S1). This trend indicates that UHRF1 expression correlates with the progression of CEWH. These results suggest that UHRF1 may have a crucial role in regulating CEWH.

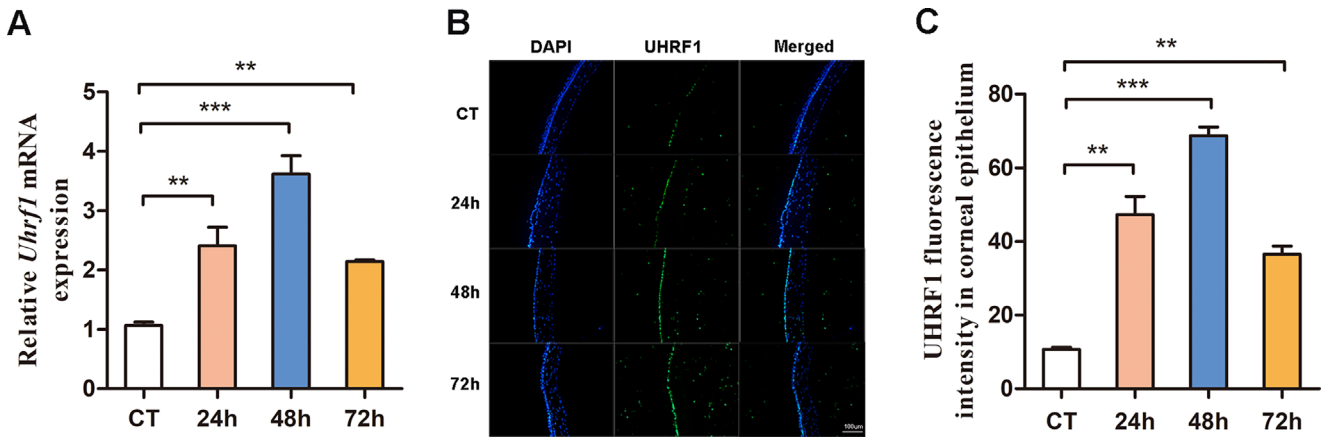

Figure 1. The spatiotemporal expression patterns of UHRF1 during CEWH. (**A**) RT-qPCR analysis of *Uhrf1* mRNA levels in mouse corneal epithelium collected at different time points (0 hours, 24 hours, 48 hours, and 72 hours) during wound healing ($n = 4$/group). Control (CT) indicates the 0 hour time point. (**B**) Representative immunofluorescence images of corneal sections stained with UHRF1 (*green*) and DAPI (*blue*) at 0 hours, 24 hours, 48 hours, and 72 hours after injury. CT indicates the 0 hour time point. (**C**) Quantitative analysis of UHRF1 relative fluorescence intensity in the corneal epithelium ($n = 4$/group). CT indicates the 0 hour time point.

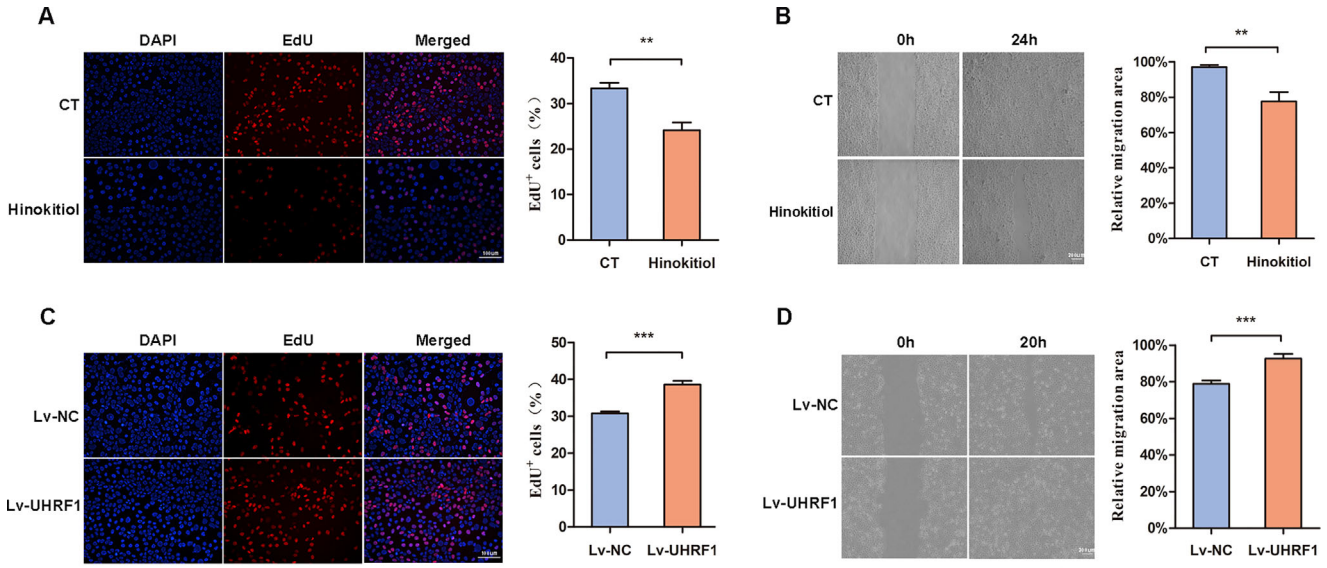

Figure 2. UHRF1 promotes cell proliferation and migration in vitro. (**A**) Immunofluorescence images of DAPI (*blue*) and EdU (*red*) staining in control (CT) and Hinokitiol-treated HCECs. Statistical analysis of proliferating cells in the CT and Hinokitiol groups ($n = 6$ per group). (**B**) Scratch wound assay images of CT and Hinokitiol-treated HCECs at 0 hours and 24 hours. Statistical analysis of migrating cells in the CT and Hinokitiol-treated HCECs ($n = 6$ per group). (**C**) Immunofluorescence images of DAPI (*blue*) and EdU (*red*) staining in Lv-negative control (NC) and Lv-UHRF1 HCECs, along with statistical analysis of proliferating cells in each group ($n = 6$ per group). (**D**) Scratch wound images of Lv-NC and Lv-UHRF1 HCECs at 0 hours and 20 hours, along with statistical analysis of migrating cells in each group ($n = 6$/group).

UHRF1 Facilitates CEWH

Our recent study has uncovered an important role for UHRF1 to modulate CEWH in vivo.[12] To further validate the involvement of UHRF1 in CEWH, we used in vitro experiments. Hinokitol, a compound derived from Chamaecyparis obtusa, inhibits UHRF1 by binding to its SRA domain, thereby disrupting DNA methylation maintenance, and holds promise for cancer therapy and epigenetic regulation research.[23,24] Inhibition of UHRF1 using Hinokitiol significantly impaired wound closure and reduced proliferation in HCECs, as evidenced by reduced migration and proliferation rates (Figs. 2A, 2B, Supplementary Fig. S2A). Conversely, overexpression of UHRF1 enhanced cell proliferation and migration, thereby accelerating wound closure in HCECs (Figs. 2C, 2D; Supplementary Fig. S2B). Taken together, these findings robustly support the hypothesis that UHRF1 plays a promotive role in CEWH.

UHRF1 Maintains DNA Methylation in CEWH

Previous research has demonstrated that DNA methylation, mediated by DNA methyltransferase 1 (DNMT1), enhances CEWH.[9] UHRF1 is known to cooperate with DNMT1 to maintain DNA methylation patterns.[25] To explore whether UHRF1 is associated with DNA methylation during CEWH, we utilized the dot blot technique. Results showed that

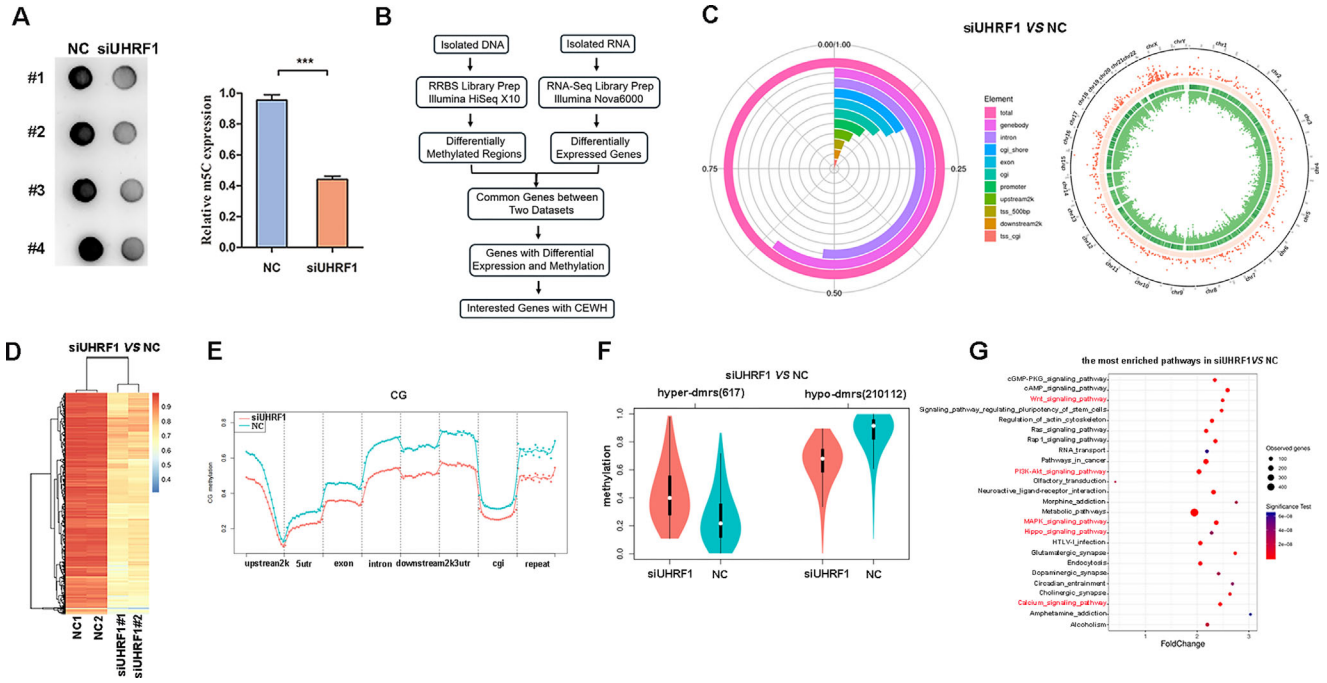

Figure 3. RRBS analysis shows decreased DNA methylation in UHRF1 knockdown HCECs. (**A**) Dot blot analysis of DNA m^5C modification following knockdown with either negative control (NC) or UHRF1 siRNA ($n = 4$ per group). (**B**) Schematic representation of the RRBS sequencing workflow. (**C**) Distribution of differential DMRs across various genomic elements. The circus plot illustrates the genomic distribution of DMRs. (**D**) Heatmap of DMRs comparing NC and siUHRF1 groups. (**E**) Average CpG methylation levels across the genome in NC and siUHRF1 HCECs. (**F**) DNA methylation levels of hypermethylated and hypomethylated CpGs within DMRs for NC and siUHRF1 groups. (**G**) KEGG enrichment analysis for differentially expressed genes within DMRs, with signaling pathways related to CEWH *highlighted in red*.

silencing UHRF1 led to a reduction in global DNA methylation levels, whereas UHRF1 overexpression increased methylation levels (Fig. 3A, Supplementary Fig. S3). RRBS provided a comprehensive view of DMRs in UHRF1-silenced HCECs (Fig. 3B). As shown in Figure 3C, UHRF1 silencing resulted in significant hypomethylation across various genomic elements, such as promoters, exons, and introns. In particular, UHRF1 knockdown significantly reduced the whole DNA methylation levels (Figs. 3D, 3E). Notably, 210,112 DMRs were hypomethylated, whereas only 617 DMRs were hypermethylated (Fig. 3F). GO analysis revealed that these differentially methylated genes were enriched in pathways crucial for CEWH,[26–30] such as the WNT, PI3K-AKT, MAPK, and Hippo signaling pathways (Fig. 3G). Taken together, these results highlight UHRF1's role in maintaining DNA methylation during CEWH.

Multi-Omics Reveals RHOB as a Potential Target of UHRF1 in CEWH

To clarify how UHRF1 modulates CEWH, we previously performed NanoString analyses to detect transcript-level changes underlying CEWH. Here, we used RNA-Seq to investigate the effects of UHRF1 silencing on mRNAs expression. Subsequently, RRBS was used to assess the impact of UHRF1 silencing on DNA methylation level. To further refine our analysis of UHRF1 targets involved in regulating CEWH, we overlapped significantly hypomethylated genes (adjusted $P < 0.05$) with significantly upregulated genes (fold change > 2; adjusted $P < 0.05$) under the UHRF1 knockdown with significantly downregulated genes ($|\text{fold change}| > 2$) during the CEWH process (Fig. 4A, Supplementary Table S1). This analysis identified 10 genes (*MUC4*, *WNT5A*, *SYT8*, *TCN2*, *CYP26B1*, *KIF26A*, *MEST*, *CRYAB*, *CRLF1*, and *RHOB*) as potential targets modulated by UHRF1 via promoter DNA methylation. Among these, *RHOB* functions as a tumor suppressor known to participate in diverse cellular activities, including cell proliferation, migration, adhesion, cytokinesis, differentiation, and apoptosis.[31] To confirm whether UHRF1 directly regulates *RHOB* expression, we performed Western blot and RT-qPCR analyses in both in vivo and in vitro models. We found that UHRF1 was significantly upregulated in CEWH, whereas RHOB was downregulated. In contrast, in vitro knockdown of UHRF1 led to a significant increase in *RHOB* expression. These results demonstrated a negative correlation between RHOB and UHRF1 expression (Figs. 4B, 4C). Subsequently, we knocked down RHOB to evaluate its functional role in CEWH. As shown in Figures 5A and 5B, RHOB knockdown significantly enhanced HCEC proliferation and migration. Furthermore, rescue experiments revealed that RHOB knockdown inhibited the increase in RHOB expression levels (Fig. 5C) and partially reversed the decrease in cell proliferation and migration induced by UHRF1 silencing in HCECs (Figs. 5D, 5E). These data highlight that RHOB is a downstream target of UHRF1 in CEWH.

UHRF1-Dependent DNA Methylation Targets RHOB

RRBS results indicated that UHRF1 silencing reduced methylation levels at the RHOB promoter (Figs. 6A, 6B). To

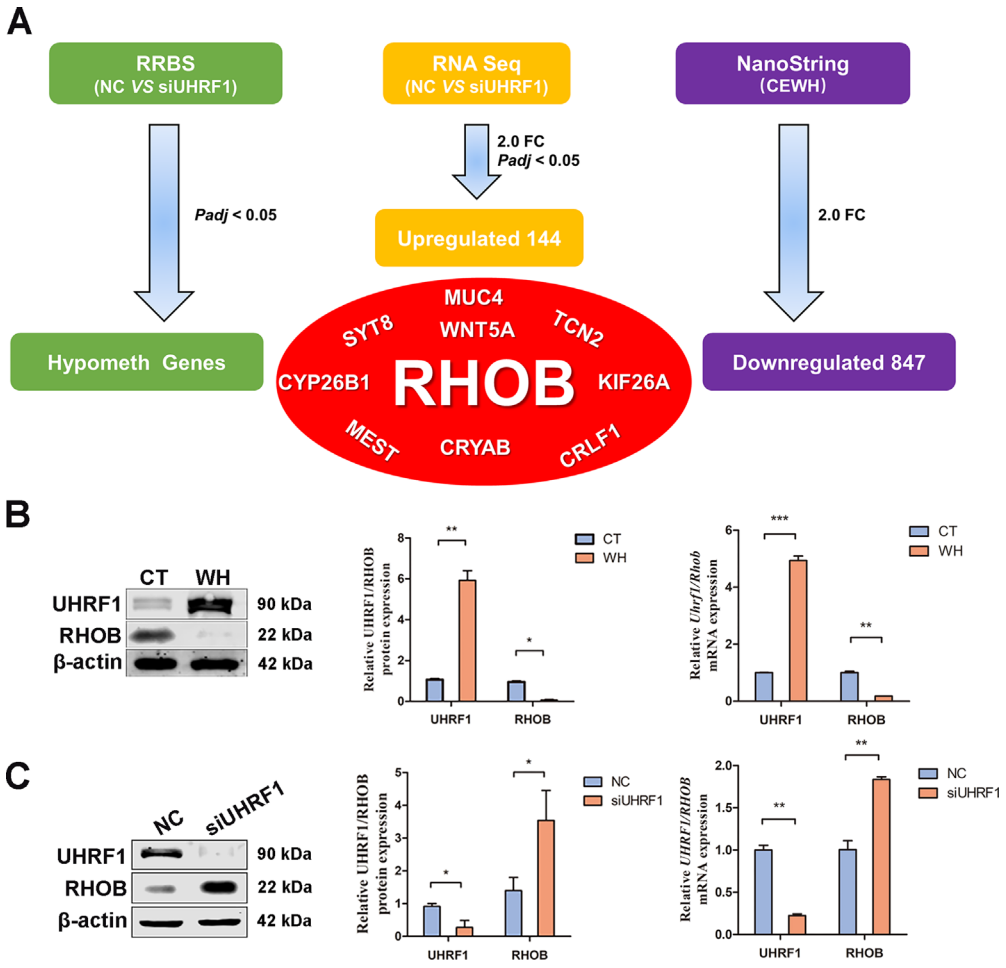

Figure 4. Multi-omics analysis identifying RHOB as a downstream target of UHRF1. (**A**) Schematic outlining the selection process for identifying direct downstream targets of UHRF1. The mouse corneal epithelium was debrided to create a CEWH model. After 48 hours, the epithelium was collected for NanoString analysis. HCECs were transfected with siRNA targeting UHRF1 for 48 hours, and the cells were then harvested for RNA-Seq or RRBS analysis. (**B**) Protein levels of UHRF1 and RHOB, along with *Uhrf1* and *Rhob* mRNA expression levels, in CEWH ($n = 3$/group). CT indicates the healthy control group. (**C**) RHOB protein levels and mRNA expression in UHRF1 knockdown HCECs ($n = 4$/group). NC indicates the negative control group.

further verify RHOB promoter DNA methylation levels, we designed five primers for targeted bisulfite sequencing (TBS; Fig. 6C, Supplementary Table S2). Two out of the five primers confirmed that UHRF1 silencing decreased promoter DNA methylation levels of RHOB (Fig. 6D, Supplementary Table S3). To investigate how DNA methylation regulates RHOB, we examined the effects of 5-Azacytidine, an inhibitor of DNA methylation, on RHOB expression in HCECs. As shown in Figures 6E and 6F, treatment with 5-Azacytidine resulted in elevated RHOB mRNA and protein expression levels compared to the control group. Collectively, these findings support the involvement of a novel UHRF1/m^{5}C-RHOB axis in CEWH.

ALYREF Regulates UHRF1 Expression in an RNA m^{5}C Dependent Manner

Our previous study demonstrated that RNA m^{5}C modification of UHRF1 plays a critical role in controlling CEWH through its interaction with ALYREF.[12] However, the mechanism by which ALYREF recognizes UHRF1 remains to be determined. To investigate this, a mutant ALYREF construct with a key amino acid mutation (K171A) to abolish its m^{5}C binding site was transfected into HEK293 cells (Fig. 7A). As shown in Figures 7B and C, an increased protein level of UHRF1 observed in the ALYREF WT group was eliminated in ALYREF MUT because of the RNA m^{5}C reader activity deficiency, but UHRF1 mRNA expression was comparable between ALYRE WT and ALYREF Mut groups. Furthermore, we also constructed UHRF1 mutants for a gene reporter luciferase assay (Fig. 7D). Compared to the UHRF1 WT, the UHRF1 MUT showed no response to ALYREF knockdown, suggesting that RNA m^{5}C modification is essential for ALYREF-mediated regulation (Fig. 7D). Most importantly, ALYREF silencing in HCECs significantly reduced the UHRF1 protein levels, whereas the RHOB protein levels increased significantly (Fig. 7E). Taken together, these results establish a novel ALYREF/UHRF1/RHOB signaling axis involved in CEWH.

Commonality of the ALYREF/UHRF1/RHOB Axis in Epithelial-Origin Tumors

As approximately 90% of all human cancers originate from epithelial cells,[20] we posed the question: could this novel ALYREF/UHRF1/RHOB axis be a common feature in epithe-

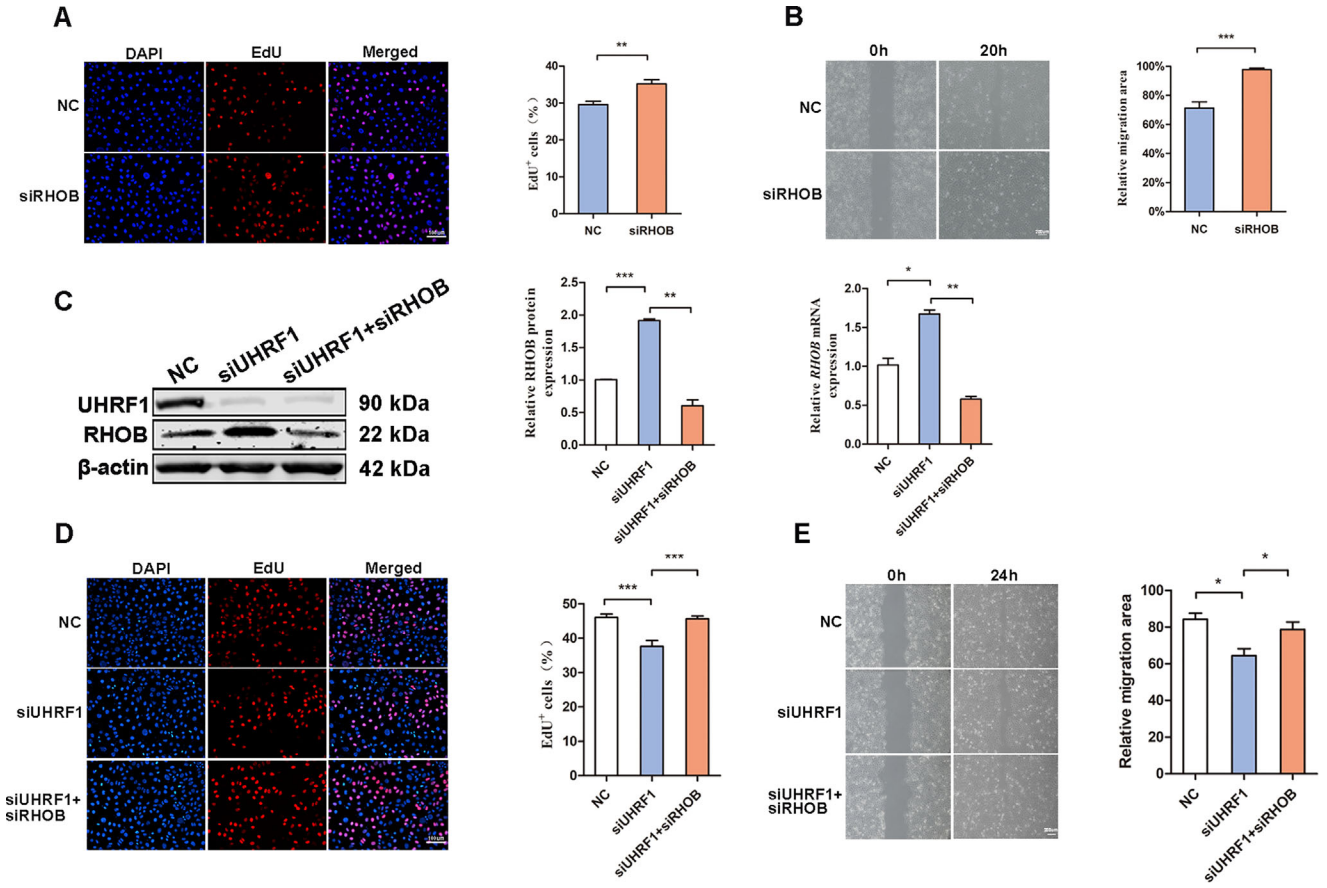

Figure 5. RHOB silencing ameliorates the suppressive effects of UHRF1 knockdown on HCEC proliferation and migration. (**A**) Immunofluorescence images showing DAPI (*blue*) and EdU (*red*) staining in the negative control group (NC) and siRHOB HCECs, with statistical analysis of proliferating cells in each group ($n = 6$/group). (**B**) Scratch wound assay images of NC and siRHOB HCECs at 0 hours and 20 hours, with statistical analysis of migrating cells in each group ($n = 6$/group). NC indicates the negative control group. (**C**) Western blot analysis of RHOB and UHRF1 protein levels in UHRF1-silenced HCECs following RHOB knockdown, with densitometric quantification of RHOB expression levels, normalized to β-actin ($n = 3$/group). RT-qPCR analysis of *RHOB* mRNA expression, also normalized to β-actin ($n = 3$/group). NC indicates the negative control group. (**D**) EdU assay assessing proliferation in UHRF1-silenced HCECs following RHOB knockdown, with statistical analysis of proliferating cells in each group ($n = 6$/group). NC indicates the negative control group. (**E**) Scratch wound assay evaluating migration in UHRF1-silenced HCECs following RHOB knockdown, with statistical analysis of migrating cells in each group ($n = 6$/group). NC indicates the negative control group.

lial tumors? To investigate, we utilized gene expression profiling interactive analysis (GEPIA) to test the hypothesis that the ALYREF/UHRF1 and UHRF1/RHOB signaling axes play a pivotal role in epithelial tumors. Correlation analyses revealed a positive correlation between ALYREF and UHRF1 expression in 21 different epithelial tumor types, whereas a negative correlation was observed between UHRF1 and RHOB expression in 13 epithelial tumors (Supplementary Figs. S4, S5). Furthermore, we used GEPIA to examine the expression levels of ALYREF, UHRF1, and RHOB in breast cancer (1085 tumors versus 291 healthy samples). As shown in Figure 8A, ALYREF and UHRF1 were significantly upregulated, whereas RHOB was downregulated in breast cancer samples. To further validate this ALYREF/UHRF1/RHOB axis, we conducted RNA interference experiments in two breast cancer cell lines, where ALYREF knockdown led to a significant increase in RHOB expression and a decrease in UHRF1 expression in both cell lines (Figs. 8B, 8C). Collectively, these findings provide evidence that this novel signaling axis is present in representative epithelial-origin tumors.

Discussion

Epigenetics involves the study of how environmental, developmental, and nutritional cues impact gene expression without altering the DNA sequence.[32] Instead, these factors influence phenotypic expression and metabolic processes by modulating DNA methylation, histone modifications, and non-coding RNA regulation.[7] Compelling evidence indicates that epigenetic mechanisms control the timing and outcome of CEWH.[8–12] Among these findings, DNA methylation has been identified as a key modulator of HCEC proliferation and migration.[9] RNA modifications, histone methylation status, and changes in the non-coding RNA expression profile also influence the outcome of CEWH.[10–12] In this study, we focus on elucidating the effects and mechanisms by which UHRF1 modulates CEWH. Furthermore, our results identify a novel epigenetic ALYREF/UHRF1/RHOB axis that regulates CEWH. Our findings underscore the critical role of epigenetic crosstalk between DNA methylation and RNA modification in controlling CEWH.

Investigative Ophthalmology & Visual Science

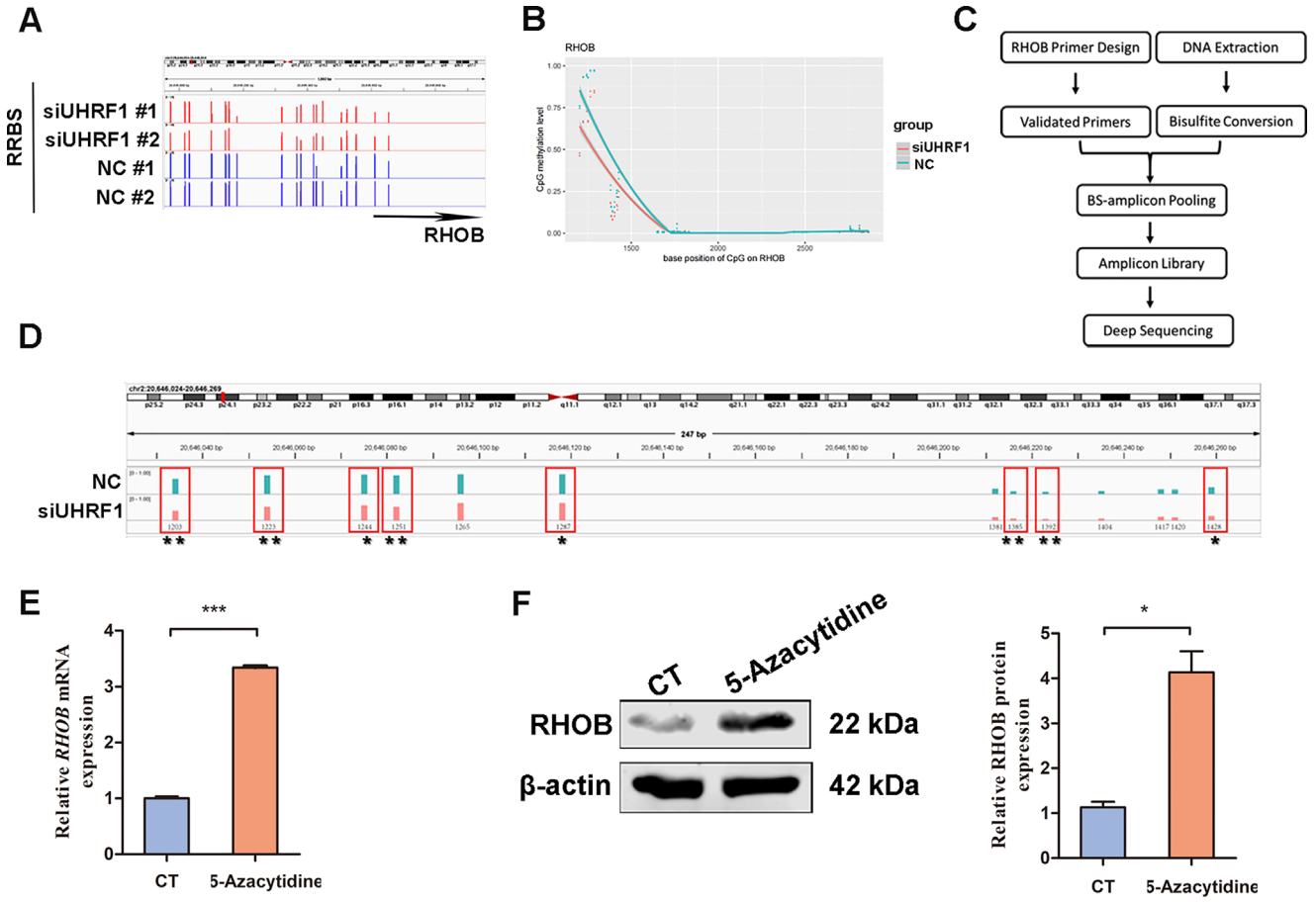

Figure 6. UHRF1 negatively modulates RHOB gene expression via promoter DNA methylation. (**A**) Integrative Genomics Viewer (IGV) analysis showing different methylation patterns in the promoter region of the RHOB gene. (**B**) Comparison of CpG methylation levels in the RHOB promoter region between the negative control (NC) and the siUHRF1 groups. (**C**) Schematic representation of the TBS sequencing workflow. (**D**) IGV analysis displaying various methylation sites in the promoter region of the *RHOB* gene and the average methylation ratio in 13 CpG sites in the histograms, of which 8 (methylation sites: 1203, 1223, 1244, 1251, 1287, 1385, 1392, and 1428) were significantly decreased in the siUHRF1 groups compared with the negative control (NC) groups. The methylation level significance is denoted with the indicated number of asterisks (*$P < 0.05$, **$P < 0.01$). (**E**) RT-qPCR analysis of *RHOB* mRNA levels in HCECs treated with the DNA methylation inhibitor 5-Azacytidine ($n = 3$/group). CT indicates the control group. (**F**) Western blot analysis showing RHOB protein levels in HCECs treated with 5-Azacytidine ($n = 3$/group). CT indicates the control group.

UHRF1, initially identified as a nuclear protein in 1998, has been recognized for its potential as an epigenetic integrator involved in various biological processes, including tissue regeneration and malignancy.[12,15] To accurately characterize the spatial expression of UHRF1 in the central cornea during CEWH, we performed immunofluorescence (IF) microscopy at 63 × oil magnification using a Zeiss LSM 880 confocal laser scanning microscope. Our results confirm that UHRF1 is predominantly localized to basal corneal epithelial cells, rather than superficial corneal epithelial cells. The specific expression of UHRF1 in basal corneal epithelial cells, as opposed to its absence in terminally differentiated superficial corneal epithelial cells, may play a crucial role in CEWH.[4,33] Furthermore, we demonstrate that the temporal patterns of UHRF1 during CEWH follow a distinct trend, with levels initially rising and subsequently declining. This pattern coincides with accelerated CEWH and increased DNA methylation.[9] Specifically, UHRF1 expression and DNA methylation levels significantly increased at 24 hours post-injury, reaching a peak at 48 hours. The time-dependent increase in UHRF1 expression observed here is consistent with our previous findings on elevated DNA methylation during CEWH. This correlation suggests that UHRF1 mediates the maintenance of DNA methylation and modulates CEWH through its effects on DNA methylation dynamics.

On the other hand, UHRF1 silencing altered the DNA methylation status of various annotated genes in HCECs. These changes were enriched in key components of the WNT, PI3K-AKT, MAPK, Hippo, and calcium signaling pathways, all of which are known to contribute to CEWH.[26–30] This finding suggests that UHRF1-mediated DNA methylation maintenance plays a role in supporting CEWH. However, UHRF1 is structurally composed of five domains: UBL, TTD, PHD, SRA, and RING.[34] Our study specifically focuses on the role of the SRA domain in UHRF1-mediated DNA methylation maintenance and its regulation of CEWH. The molecular basis of this process is primarily attributed to the following mechanisms: The SRA domain of UHRF1 is essential for maintaining DNA methylation, as it has the unique ability to recognize hemimethylated CpG sites.[14] This recognition facilitates the recruitment of DNMT1, the prin-

Investigative Ophthalmology & Visual Science

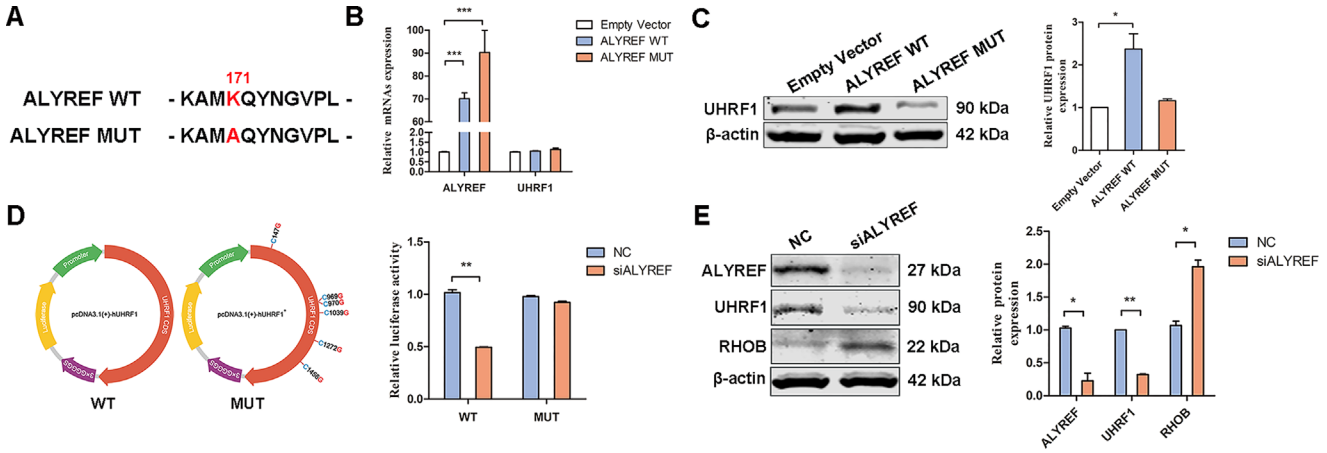

Figure 7. ALYREF positively regulates UHRF1 expression in an RNA m^5C-dependent manner. (**A**) Schematic of the ALYREF wild type (WT) and ALYREF mutant (MUT; K171A). (**B**) RT-qPCR analysis of *ALYREF* and *UHRF1* mRNA expression, normalized to β-actin ($n = 3$/group). (**C**) Western blot analysis of UHRF1 protein levels in ALYREF WT- or ALYTEF MUT-transfected HEK293 cells, with densitometric quantification of UHRF1 expression levels, normalized to β-actin ($n = 3$/group). (**D**) Schematic representation of the experimental design: WT or MUT UHRF1-CDS sequences were fused with a firefly luciferase reporter. The MUT UHRF1-CDS sequence contains modifications at m^5C sites (C to G substitutions at positions 147, 969, 970, 1039, 1272, and 1456) within the coding sequence of the pcDNA 3.1 vector, allowing investigation of RNA m^5C's role in UHRF1 expression. Luciferase reporter assay measuring luciferase activity in HEK293 cells transfected with WT or MUT UHRF1-CDS under ALYREF knockdown conditions ($n = 3$/group). (**E**) Western blot analysis of ALYREF, UHRF1, and RHOB protein levels in ALYREF-silenced HCECs ($n = 3$/group). NC indicates the negative control group.

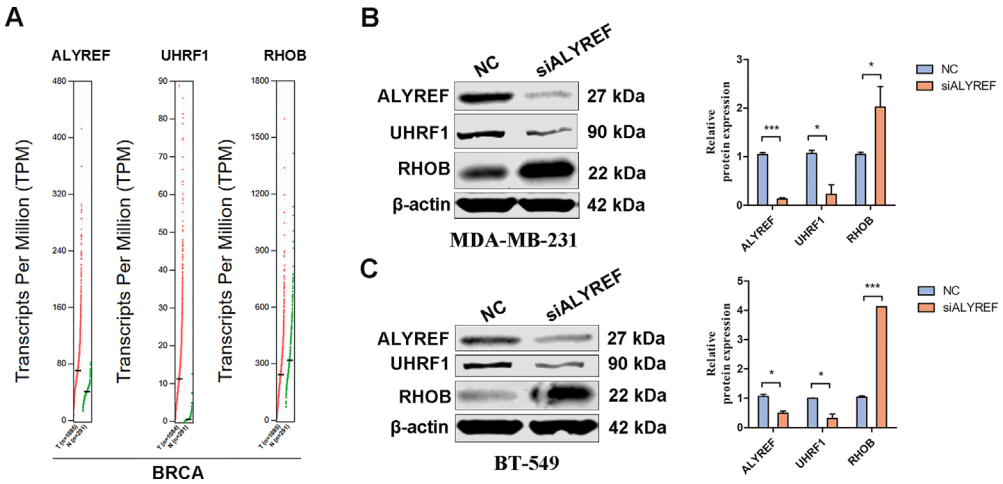

Figure 8. Presence of the epigenetic ALYREF/UHRF1/RHOB axis in breast cancer (BRCA). (**A**) GEPIA analysis shows upregulation of ALYREF and UHRF1, and downregulation of RHOB in BRCA. (**B**) Western blot analysis of ALYREF, UHRF1, and RHOB protein levels in the MDA-MB-231 cell line following ALYREF silencing ($n = 3$/group). (**C**) Western blot analysis of ALYREF, UHRF1, and RHOB protein levels in the BT-549 cell line following ALYREF silencing ($n = 3$/group). NC indicates the negative control group.

cipal maintenance methyltransferase, ensuring the precise methylation of newly synthesized DNA strands.[35] Moreover, the SRA domain is involved in the regulation of histone modifications, which in turn establishes a favorable environment for DNMT1 activity.[36] Its structural specificity and the coordinated regulation of both DNA and histone methylation make it indispensable for maintaining epigenetic stability, especially in CEWH, where UHRF1 overexpression is a well-documented phenomenon. The functions of the other UHRF1 domains and their potential involvement in CEWH through alternative regulatory mechanisms remain beyond the scope of the current study and warrant further investigation.

Building on these findings, we conducted a multi-omics analysis that revealed that UHRF1 promotes CEWH by downregulating RHOB, a member of the RHO GTPase family and a known tumor suppressor involved in various cellular processes, including cell proliferation, migration, division, and adhesion.[37] In this study, the UHRF1-induced enhancement of the wound healing response was associated with RHOB downregulation and increased DNA methylation at the RHOB promoter. UHRF1 regulates DNA methylation at the RHOB promoter through a combination of mechanisms, including recognizing hemimethylated DNA, recruiting and activating DNMT1, modifying histones, and interacting with other epigenetic regulators. This precise

Investigative Ophthalmology & Visual Science

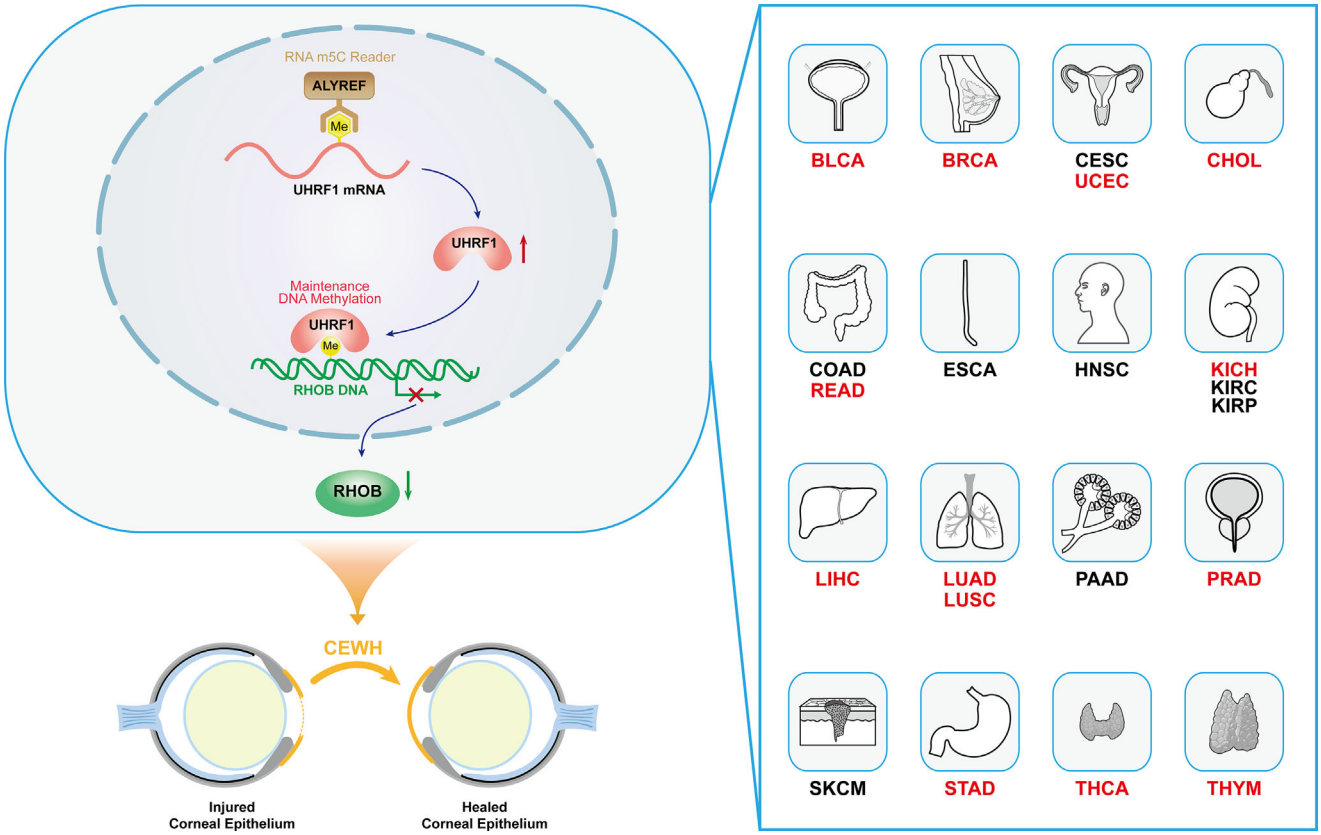

Figure 9. Schematic model of the novel epigenetic ALYREF/UHRF1/RHOB axis in CEWH. This model illustrates how the ALYREF/UHRF1/RHOB axis modulates CEWH and suggests its potential role in various epithelial-derived tumors.

regulation is essential for maintaining RHOB gene expression.[38,39] Our previous studies have partially supported this mechanism, particularly regarding the functional roles of DNMT1 and H3K9me3 in modulating CEWH.[9,10] Collectively, we identified a novel UHRF1/m^{5}C-RHOB signaling axis during CEWH. Despite the fact that approximately 90% of human cancers are of epithelial origin,[20] the precise contribution of this signaling axis to epithelial tumor formation remains to be fully elucidated. Some insights into this possibility are provided by our observation of a negative correlation between UHRF1 and RHOB expression in 13 epithelial-derived tumors. However, previous studies have indicated that methylation of RHOB promoter regions remains unchanged in certain cancers, such as lung cancer and ovarian carcinogenesis, as well as in various murine tissues across different ages.[40–42] Our study suggests that RHOB transcription in corneal epithelium is epigenetically regulated in a tissue-specific manner during CEWH, partially through alterations in DNA methylation. Further research is warranted to investigate the role of the UHRF1/m^{5}C-RHOB signaling axis in epithelial-derived tumors.

Our study further demonstrates that ALYREF functions as an RNA m^{5}C reader that modulates CEWH by binding to *UHRF1* mRNA. This interaction enhances the translation of *UHRF1* rather than influencing its mRNA expression in an RNA m^{5}C-dependent manner. ALYREF is frequently amplified in numerous tumors,[43,44] and positive correlations between ALYREF and UHRF1 expression have been observed across 21 epithelial-derived tumors. Notably, UHRF1 expression is regulated by RNA m^{5}C modification, and UHRF1, in turn, mediates promoter DNA methylation of RHOB, suggesting that UHRF1 serves as an epigenetic crosstalk hub connecting RNA m^{5}C modification to DNA methylation. Furthermore, UHRF1 is recognized as a universal biomarker for cancers.[45] We also demonstrated that silencing ALYREF significantly reduced UHRF1 levels while increasing RHOB levels in two breast cancer cell lines. These results highlight the presence of the ALYREF/UHRF1/RHOB axis in epithelial cancer. To assess the broader relevance of this axis, we analyzed mRNA expression and overall survival using TCGA RNA-Seq data. The results revealed that both ALYREF and UHRF1 were upregulated, whereas RHOB was downregulated, and all three were correlated with overall survival (data not shown). This supports the universal significance of the ALYREF/UHRF1/RHOB axis in epithelial cancer. Furthermore, it has been established that UHRF1 is an oncogene, whereas RHOB acts as a tumor suppressor.[19,31] ALYREF, on the other hand, is overexpressed in all epithelial cancers, with growing evidence suggesting that its overexpression drives tumorigenesis.[43,44] Thus, we speculate that overexpression of ALYREF or UHRF1, coupled with low expression of RHOB, could influence epithelial tumorigenesis. These findings imply that targeting the ALYREF/UHRF1/RHOB axis may help prevent the development of epithelial cancers. Collectively, these findings from the well-established CEWH model have broader implications, pointing to a potential role for RNA m^{5}C-targeted therapies in treating wound healing-associated phenotypes and the 90% of human cancers that originate from epithelial cells.[20]

Interestingly, our previous research in uveal melanoma (UM) demonstrated that miR-124a expression is silenced by DNA methylation.[46] The silencing of miR-124a upregulates its downstream target, NSUN2, resulting in enhanced RNA m^5C methylation, which in turn promotes malignant biological behaviors in UM cells, such as proliferation and migration.[47] In short, this represents a model in UM in which DNA methylation regulates RNA m^5C methylation. In contrast, the present study identified an inverse regulatory model through the ALYREF/UHRF1/RHOB axis, with regulation proceeding from RNA m^5C methylation to DNA methylation. These findings highlight a dynamic crosstalk between DNA methylation and RNA m^5C methylation, implying that the directionality of this regulation can vary depending on the biological context, such as differing ocular diseases. Determining the factors that govern this regulatory direction warrants further investigation.

In summary, we identified a previously unexplored epigenetic ALYREF/UHRF1/RHOB axis, which facilitates CEWH. Even though the cornea is only part of such a small biological realm, this epigenetic axis stems from corneal epithelium could have broader applicability in most epithelial derived tumors (Fig. 9).

Acknowledgments

The authors thank the GEPIA for providing open access.

Supported, in part, by the National Natural Science Foundation of China (82371031 and 81900818), the Zhejiang Provincial Natural Science Foundation of China (LZ23H160002, LQ24H120005, and LY21H120005), and the Foundation of Wenzhou Science & Technology Bureau (H20220009).

Disclosure: **H. Zhang**, None; **S. Lan**, None; **D. Ren**, None; **X. Chen**, None; **Y. Lin**, None; **Q. Cao**, None; **W. Xu**, None; **J. Wang**, None; **P. Sol Reinach**, None; **D. Yan**, None; **G. Luo**, None

References

1. Ljubimov AV, Saghizadeh M. Progress in corneal wound healing. *Prog Retin Eye Res*. 2015;49:17–45.
2. Leong YY, Tong L. Barrier function in the ocular surface: from conventional paradigms to new opportunities. *Ocul Surf*. 2015;13:103–109.
3. Fortingo N, Melnyk S, Sutton SH, Watsky MA, Bollag WB. Innate immune system activation, inflammation and corneal wound healing. *Int J Mol Sci*. 2022;23:14933.
4. Altshuler A, Amitai-Lange A, Tarazi N, et al. Discrete limbal epithelial stem cell populations mediate corneal homeostasis and wound healing. *Cell Stem Cell*. 2021;28:1248–1261.e1248.
5. Lin JB, Shen X, Pfeifer CW, et al. Dry eye disease in mice activates adaptive corneal epithelial regeneration distinct from constitutive renewal in homeostasis. *Proc Natl Acad Sci USA*. 2023;120:e2204134120.
6. Wirostko B, Rafii M, Sullivan DA, Morelli J, Ding J. Novel therapy to treat corneal epithelial defects: a hypothesis with growth hormone. *Ocul Surf*. 2015;13:204–212.e201.
7. Cavalli G, Heard E. Advances in epigenetics link genetics to the environment and disease. *Nature*. 2019;571:489–499.
8. Chen E, Bohm K, Rosenblatt M, Kang K. Epigenetic regulation of anterior segment diseases and potential therapeutics. *Ocul Surf*. 2020;18:383–395.
9. Luo G, Jing X, Yang S, et al. DNA methylation regulates corneal epithelial wound healing by targeting miR-200a and CDKN2B. *Invest Ophthalmol Vis Sci*. 2019;60:650–660.
10. Yang S, Chen W, Jin S, et al. SUV39H1 regulates corneal epithelial wound healing via H3K9me3-mediated repression of p27. *Eye Vis (Lond)*. 2022;9:4.
11. An J, Chen X, Chen W, et al. MicroRNA expression profile and the role of miR-204 in corneal wound healing. *Invest Ophthalmol Vis Sci*. 2015;56:3673–3683.
12. Luo G, Xu W, Chen X, et al. The RNA m5C methylase NSUN2 modulates corneal epithelial wound healing. *Invest Ophthalmol Vis Sci*. 2023;64:5.
13. Rottach A, Frauer C, Pichler G, Bonapace IM, Spada F, Leonhardt H. The multi-domain protein Np95 connects DNA methylation and histone modification. *Nucleic Acids Res*. 2010;38:1796–1804.
14. Bostick M, Kim JK, Esteve PO, Clark A, Pradhan S, Jacobsen SE. UHRF1 plays a role in maintaining DNA methylation in mammalian cells. *Science*. 2007;317:1760–1764.
15. Fujimori A, Matsuda Y, Takemoto Y, et al. Cloning and mapping of Np95 gene which encodes a novel nuclear protein associated with cell proliferation. *Mamm Genome*. 1998;9:1032–1035.
16. Wang S, Zhang C, Hasson D, et al. Epigenetic compensation promotes liver regeneration. *Dev Cell*. 2019;50:43–56.e46.
17. Kostyrko K, Roman M, Lee AG, et al. UHRF1 is a mediator of KRAS driven oncogenesis in lung adenocarcinoma. *Nat Commun*. 2023;14:3966.
18. Mudbhary R, Hoshida Y, Chernyavskaya Y, et al. UHRF1 overexpression drives DNA hypomethylation and hepatocellular carcinoma. *Cancer Cell*. 2014;25:196–209.
19. Kim A, Benavente CA. Oncogenic roles of UHRF1 in cancer. *Epigenomes*. 2024;8:26.
20. Bray F, Ferlay J, Soerjomataram I, Siegel RL, Torre LA, Jemal A. Global cancer statistics 2018: GLOBOCAN estimates of incidence and mortality worldwide for 36 cancers in 185 countries. *CA Cancer J Clin*. 2018;68:394–424.
21. Yang X, Yang Y, Sun BF, et al. 5-methylcytosine promotes mRNA export - NSUN2 as the methyltransferase and ALYREF as an m(5)C reader. *Cell Res*. 2017;27:606–625.
22. Gao F, Liang H, Lu H, et al. Global analysis of DNA methylation in hepatocellular carcinoma by a liquid hybridization capture-based bisulfite sequencing approach. *Clin Epigenetics*. 2015;7:86.
23. Seo JS, Choi YH, Moon JW, Kim HS, Park SH. Hinokitiol induces DNA demethylation via DNMT1 and UHRF1 inhibition in colon cancer cells. *BMC Cell Biol*. 2017;18:14.
24. Wang Y, Hu P, Wang F, et al. UHRF1 inhibition epigenetically reprograms cancer stem cells to suppress the tumorigenic phenotype of hepatocellular carcinoma. *Cell Death Dis*. 2023;14:381.
25. Li T, Wang L, Du Y, et al. Structural and mechanistic insights into UHRF1-mediated DNMT1 activation in the maintenance DNA methylation. *Nucleic Acids Res*. 2018;46:3218–3231.
26. Nakatsu MN, Ding Z, Ng MY, Truong TT, Yu F, Deng SX. Wnt/beta-catenin signaling regulates proliferation of human cornea epithelial stem/progenitor cells. *Invest Ophthalmol Vis Sci*. 2011;52:4734–4741.
27. Mao Y, Ou S, Zhu C, et al. Downregulation of p38 MAPK signaling pathway ameliorates tissue-engineered corneal epithelium. *Tissue Eng Part A*. 2022;28:977–989.
28. Chen K, Li Y, Zhang X, Ullah R, Tong J, Shen Y. The role of the PI3K/AKT signalling pathway in the corneal epithelium: recent updates. *Cell Death Dis*. 2022;13:513.
29. Hou L, Fu W, Liu Y, Wang Q, Wang L, Huang Y. Agrin promotes limbal stem cell proliferation and corneal wound healing through hippo-yap signaling pathway. *Invest Ophthalmol Vis Sci*. 2020;61:7.

30. Sun CC, Lee SY, Chen LH, et al. Targeting Ca(2+)-dependent pathways to promote corneal epithelial wound healing induced by CISD2 deficiency. *Cell Signal*. 2023;109:110755.
31. Prendergast GC. Actin' up: RhoB in cancer and apoptosis. *Nat Rev Cancer*. 2001;1:162–168.
32. Feil R, Fraga MF. Epigenetics and the environment: emerging patterns and implications. *Nat Rev Genet*. 2012;13:97–109.
33. Ramesh V, Bayam E, Cernilogar FM, et al. Loss of Uhrf1 in neural stem cells leads to activation of retroviral elements and delayed neurodegeneration. *Genes Dev*. 2016;30:2199–2212.
34. Mancini M, Magnani E, Macchi F, Bonapace IM. The multi-functionality of UHRF1: epigenome maintenance and preservation of genome integrity. *Nucleic Acids Res*. 2021;49:6053–6068.
35. Avvakumov GV, Walker JR, Xue S, et al. Structural basis for recognition of hemi-methylated DNA by the SRA domain of human UHRF1. *Nature*. 2008;455:822–825.
36. Johnson LM, Bostick M, Zhang X, et al. The SRA methylcytosine-binding domain links DNA and histone methylation. *Curr Biol*. 2007;17:379–384.
37. Vega FM, Ridley AJ. The RhoB small GTPase in physiology and disease. *Small GTPases*. 2018;9:384–393.
38. Liu X, Gao Q, Li P, et al. UHRF1 targets DNMT1 for DNA methylation through cooperative binding of hemi-methylated DNA and methylated H3K9. *Nat Commun*. 2013;4:1563.
39. Oh YM, Mahar M, Ewan EE, Leahy KM, Zhao G, Cavalli V. Epigenetic regulator UHRF1 inactivates REST and growth suppressor gene expression via DNA methylation to promote axon regeneration. *Proc Natl Acad Sci USA*. 2018;115:E12417–E12426.
40. Mazieres J, Tovar D, He B, et al. Epigenetic regulation of RhoB loss of expression in lung cancer. *BMC Cancer*. 2007;7:220.
41. Yoon YS, Choo JH, Yoo T, Kang K, Chung JH. RhoB is epigenetically regulated in an age- and tissue-specific manner. *Biochem Biophys Res Commun*. 2007;362:164–169.
42. Liu Y, Song N, Ren K, et al. Expression loss and revivification of RhoB gene in ovary carcinoma carcinogenesis and development. *PLoS One*. 2013;8:e78417.
43. Nagy Z, Seneviratne JA, Kanikevich M, et al. An ALYREF-MYCN coactivator complex drives neuroblastoma tumorigenesis through effects on USP3 and MYCN stability. *Nat Commun*. 2021;12:1881.
44. Klec C, Knutsen E, Schwarzenbacher D, et al. ALYREF, a novel factor involved in breast carcinogenesis, acts through transcriptional and post-transcriptional mechanisms selectively regulating the short NEAT1 isoform. *Cell Mol Life Sci*. 2022;79:391.
45. Ashraf W, Ibrahim A, Alhosin M, et al. The epigenetic integrator UHRF1: on the road to become a universal biomarker for cancer. *Oncotarget*. 2017;8:51946–51962.
46. Chen X, He D, Dong XD, et al. MicroRNA-124a is epigenetically regulated and acts as a tumor suppressor by controlling multiple targets in uveal melanoma. *Invest Ophthalmol Vis Sci*. 2013;54:2248–2256.
47. Luo G, Xu W, Chen X, et al. NSUN2-mediated RNA m(5)C modification modulates uveal melanoma cell proliferation and migration. *Epigenetics*. 2022;17:922–933.

Investigative Ophthalmology & Visual Science